

Southern Illinois University Edwardsville

**SPARK**

---

SIUE Faculty Research, Scholarship, and Creative Activity

---

Spring 3-3-2016

## Synthesis, Structural Characterization and Catalytic Activity of Indenyl tris-N-Pyrrolyl Phosphine Complexes of Ruthenium

Matthew J. Stark

*University of Missouri-Saint Louis*

Michael J. Shaw

*Southern Illinois University at Edwardsville, michsha@siue.edu*

Nigam P. Rath

*University of Missouri-Saint Louis*

Eike B. Bauer

*University of Missouri-Saint Louis*

Follow this and additional works at: [https://spark.siue.edu/siue\\_fac](https://spark.siue.edu/siue_fac)

 Part of the [Inorganic Chemistry Commons](#)

---

### Recommended Citation

Stark, Matthew J.; Shaw, Michael J.; Rath, Nigam P.; and Bauer, Eike B., "Synthesis, Structural Characterization and Catalytic Activity of Indenyl tris-N-Pyrrolyl Phosphine Complexes of Ruthenium" (2016). *SIUE Faculty Research, Scholarship, and Creative Activity*. 30.  
[https://spark.siue.edu/siue\\_fac/30](https://spark.siue.edu/siue_fac/30)

This Article is brought to you for free and open access by SPARK. It has been accepted for inclusion in SIUE Faculty Research, Scholarship, and Creative Activity by an authorized administrator of SPARK. For more information, please contact [jkohlbu@siue.edu](mailto:jkohlbu@siue.edu).

# Synthesis, Structural Characterization and Catalytic Activity of Indenyl tris-*N*-Pyrrolyl Phosphine Complexes of Ruthenium

Matthew J. Stark,<sup>a</sup> Michael J. Shaw,<sup>b</sup> Nigam P. Rath,<sup>a,c</sup> and Eike B. Bauer<sup>a,\*</sup>

<sup>a</sup> *University of Missouri - St. Louis, Department of Chemistry and Biochemistry, One University Boulevard, St. Louis, MO 63121, USA.*

<sup>b</sup> *Southern Illinois University Edwardsville, Department of Chemistry, Edwardsville, IL 62025, USA.*

<sup>c</sup> *Center for Nanoscience, University of Missouri - St. Louis.*

[bauere@umsl.edu](mailto:bauere@umsl.edu), [www.eike-bauer.net](http://www.eike-bauer.net)

*To be submitted to the European Journal of Inorganic Chemistry*

Keywords: tris-*N*-pyrrolyl phosphine, electronic tuning, X-Ray, cyclic voltammetry, propargylic alcohols

## Abstract

The synthesis, characterization and catalytic activity of new ruthenium complexes of the tris-*N*-pyrrolyl phosphine ligand P(pyr)<sub>3</sub> is described. The new ruthenium complexes

[RuCl(ind)(PPh<sub>3</sub>){P(pyr)<sub>3</sub>}] and [RuCl(ind){P(pyr)<sub>3</sub>}<sub>2</sub>] (ind = indenyl ligand  $\eta^5\text{-C}_9\text{H}_7^-$ ) were synthesized in 73% and 63% isolated yield, respectively, by thermal ligand exchange of [RuCl(ind)(PPh<sub>3</sub>)<sub>2</sub>] with P(pyr)<sub>3</sub>. The electronic and steric properties of the new complexes were studied through analysis of the X-Ray structures and through cyclic voltammetry. The new complexes [RuCl(ind)(PPh<sub>3</sub>){P(pyr)<sub>3</sub>}] and [RuCl(ind){P(pyr)<sub>3</sub>}<sub>2</sub>] and the known complex [RuCl(ind)(PPh<sub>3</sub>)<sub>2</sub>] differed only slightly in their steric properties, as seen from the comparable bond lengths and angles around the ruthenium center. The oxidation potentials of [RuCl(ind)(PPh<sub>3</sub>){P(pyr)<sub>3</sub>}] and [RuCl(ind){P(pyr)<sub>3</sub>}<sub>2</sub>] are +0.34 and +0.71 Volt vs. Cp<sub>2</sub>Fe<sup>0/+</sup>, which are substantially higher than that of [RuCl(ind)(PPh<sub>3</sub>)<sub>2</sub>] (-0.023 V), which is in accordance with the enhanced  $\pi$ -acidity of the P(pyr)<sub>3</sub> ligand. The new complexes are catalytically active in the etherification of propargylic alcohols and in the first ruthenium-catalyzed formation of known and new xanthenones from propargylic alcohols and diketones (18 to 72 h at 90 °C in ClCH<sub>2</sub>CH<sub>2</sub>Cl or toluene, 1-2 mol-% catalyst, 69-22 % isolated yields).

## Introduction

Transition metal complexes of ruthenium are utilized in applications for broad fields such as in catalysis<sup>[1]</sup> or for optical devices.<sup>[2]</sup> In medicinal organometallic chemistry ruthenium complexes are increasingly investigated as alternative to platinum-based anti-cancer drugs (which are limited by side-effects).<sup>[1a,3,4]</sup> A plethora of ruthenium complexes is known, as are attempts to modify them in order to improve performance for their respective applications. Tuning of the electronic properties of ruthenium complexes is most commonly achieved through their ancillary ligands.<sup>[1c,4]</sup> Knowledge of the effect of ligands on

electronic (and steric) properties allows for the tailored synthesis of ruthenium complexes with unique properties for specialized applications.

Phosphines are probably still the most widely utilized ligand class in the synthesis and application of ruthenium complexes,<sup>[5]</sup> albeit other ligands such as carbenes<sup>[6]</sup> or imines<sup>[7]</sup> are increasingly utilized. Phosphine ligands bearing aryl and alkyl groups are the most common ones used in metal complex syntheses, and their electronic modification is achieved through aryl substituents or through the nature of the alkyl groups.<sup>[8]</sup> While powerful, tuning options are somewhat limited at times, as in some cases they might require lengthy syntheses, hampering practical applications. The search for readily available phosphine ligands with unique electronic properties is, thus, ongoing.

tris-*N*-Pyrrolyl phosphine is a readily accessible ligand with electronic properties different from the PPh<sub>3</sub> ligand.<sup>[9]</sup> Research in the past decade has shown that tris-*N*-pyrrolyl phosphine (herein abbreviated P(pyr)<sub>3</sub>, pyr = *N*-pyrrolyl) exhibits increased  $\pi$ -acidity<sup>[10]</sup> with electronic properties similar to CO.<sup>[9]</sup> The electron-withdrawing properties of the ligand were demonstrated through the IR  $\nu_{\text{CO}}$  stretching frequencies of its rhodium chloro carbonyl complex, which are frequently utilized to assess the electronic properties of a ligand.<sup>[9]</sup> Also, the oxidation potential, as determined by cyclic voltammetry, indicates the  $\pi$ -acidity of tris-*N*-pyrrolyl phosphine.<sup>[11]</sup> Further electronic tuning is possible by placing electron-withdrawing substituents on the pyrrolyl ring.<sup>[12]</sup> A few ruthenium complexes of tris-*N*-pyrrolyl phosphine<sup>[13]</sup> and their catalytic applications are known (Figure 1).<sup>[11]</sup> Nevertheless, the chemistry of tris-*N*-pyrrolyl phosphine complexes of ruthenium is by far less explored than that of PPh<sub>3</sub>

and its analogs. We think that improved knowledge in the coordination chemistry of that ligand will open the pathway for its use in the synthesis of tailored ruthenium complexes.

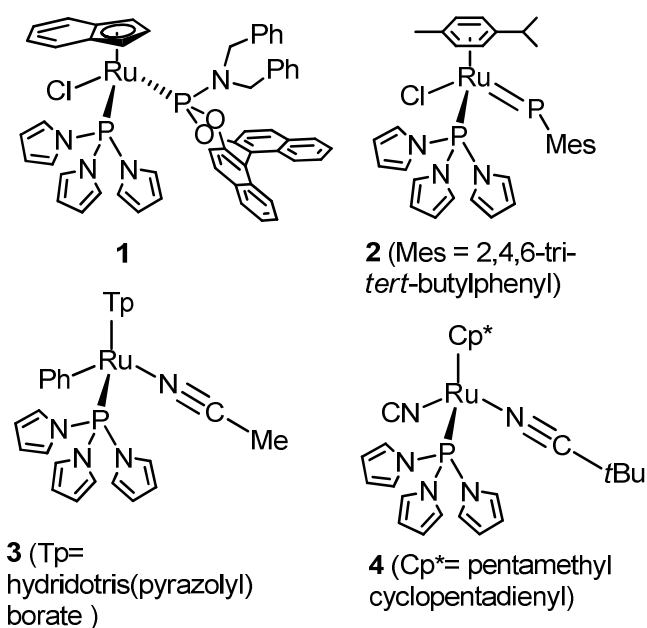


**Figure 1.** Representative tris-*N*-pyrrolyl phosphine complexes of ruthenium.

As part of our long-standing research program directed towards the catalytic activation of propargylic alcohols,<sup>[14,15]</sup> we were interested in investigating electron-poor ruthenium complexes. Propargylic alcohols can be catalytically activated by ruthenium complexes,<sup>[16]</sup> for example through the formation of ruthenium allenylidene complexes  $[\text{Ru}=\text{C}=\text{C}=\text{CR}_2]^{2+}$ <sup>[14,17]</sup> and we speculated that the reactivity of potential allenylidene intermediates with nucleophiles will increase with decreased electron-density at the metal. The known<sup>[18]</sup> ruthenium indenyl complex  $[\text{RuCl}(\text{ind})(\text{PPh}_3)_2]$  (ind =  $\eta^5\text{-C}_9\text{H}_7^-$ ) has previously been utilized as a starting material for organometallic syntheses<sup>[19]</sup> and ruthenium indenyl complexes are frequently applied in catalysis.<sup>[20]</sup> The increased reactivity of indenyl

complexes has been ascribed to the so called “indenyl effect”.<sup>[21]</sup> The formation of open coordination sites of the corresponding complexes is facilitated through an  $\eta^5$ - $\eta^3$  ring slip compared to the analogous cyclopentadienyl complexes. The effect has been ascribed through gain of aromaticity of the benzo portion of the ligand through a ring slip <sup>[21e]</sup> or related to the lower M-C bond energies of  $\eta^5$ -indenyl complexes compared to  $\eta^5$ -cyclopentadienyl.<sup>[21b]</sup> We were interested in synthesizing tris-*N*-pyrrolyl phosphine analogues of [RuCl(ind)(PPh<sub>3</sub>)<sub>2</sub>] in anticipation of accessing ruthenium complexes of increased Lewis acidity that will improve catalytic activity for the transformation of propargylic alcohols.

Herein, we describe the synthesis and characterization of the ruthenium complexes [RuCl(ind)(PPh<sub>3</sub>){P(pyr)<sub>3</sub>}] and [RuCl(ind){P(pyr)<sub>3</sub>}<sub>2</sub>]. We assess the electronic properties of the new complexes through analysis of the X-Ray structures and through cyclic voltammetry. Finally, we demonstrate that the new complexes are catalytically active in the etherification of propargylic alcohols and in the first ruthenium catalyzed formation of xanthenones from propargylic alcohols and diketones.

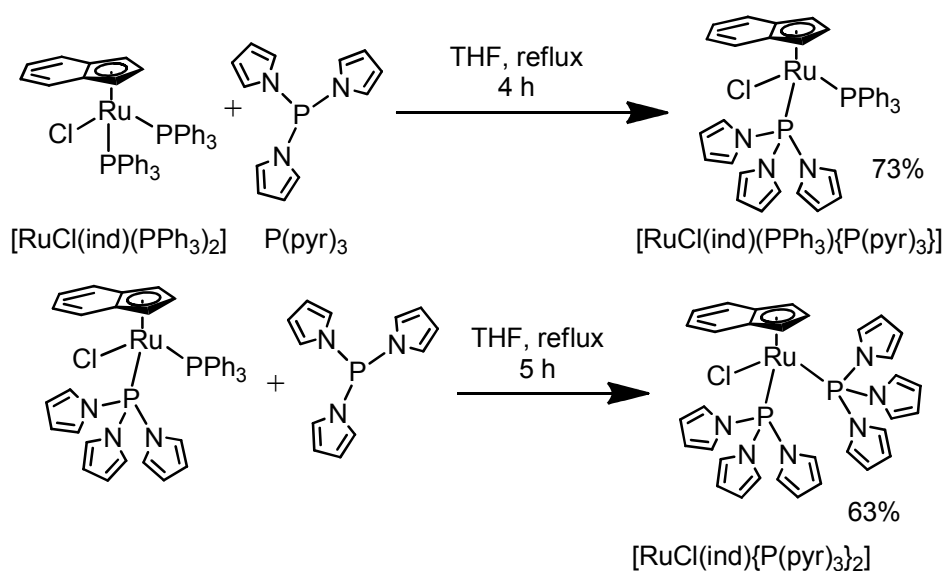
## **Results and Discussion**

### **Ligand and ruthenium complex syntheses.**

Several syntheses for the tris-*N*-pyrrolyl phosphine ligand P(pyr)<sub>3</sub> have been described in the literature.<sup>[9, 10f]</sup> We prepared the ligand through a slightly modified literature procedure,<sup>[9]</sup> which is given in the Supporting Information. In general, it is important to work under moisture-free conditions and distill all starting materials immediately prior to use.

The precursor complex [RuCl(ind)(PPh<sub>3</sub>)<sub>2</sub>] has been used as starting material for ruthenium complex syntheses through ligand substitution reactions by us <sup>[13, 14e,f]</sup> and

others.<sup>[22]</sup> Accordingly, when  $[\text{RuCl}(\text{ind})(\text{PPh}_3)_2]$  was refluxed with 1.1 equivalents of  $\text{P}(\text{pyr})_3$  in THF for 4 hours, the mono-pyrrolyl phosphine complex  $[\text{RuCl}(\text{ind})(\text{PPh}_3)\{\text{P}(\text{pyr})_3\}]$  was isolated in 73% yield as a red solid after chromatographic workup (Scheme 1). In a second ligand exchange reaction,  $[\text{RuCl}(\text{ind})(\text{PPh}_3)\{\text{P}(\text{pyr})_3\}]$  was refluxed with another equivalent of  $\text{P}(\text{pyr})_3$  in THF for 5 hours. The bis pyrrolyl phosphine complex  $[\text{RuCl}(\text{ind})\{\text{P}(\text{pyr})_3\}_2]$  was obtained in 63% yield as an orange yellow solid after column chromatography. Attempts to access  $[\text{RuCl}(\text{ind})\{\text{P}(\text{pyr})_3\}_2]$  directly from  $[\text{RuCl}(\text{ind})(\text{PPh}_3)_2]$  in a double ligand exchange reaction failed, as a mixture of the mono- and disubstituted complexes resulted, which made workup difficult and lowered the yield.



**Scheme 1.** Synthesis of tris-*N*-pyrrolyl phosphine complexes of ruthenium.

The new complexes were characterized by multinuclear NMR, MS, IR, elemental analysis and X-Ray diffraction. In the complex  $[\text{RuCl}(\text{ind})(\text{PPh}_3)\{\text{P}(\text{pyr})_3\}]$ , the coordination of one  $\text{P}(\text{pyr})_3$  and one  $\text{PPh}_3$  ligand is readily indicated by two distinct  $^{31}\text{P}\{^1\text{H}\}$  NMR signals

at 122.8 and 40.4 ppm, which exhibited a coupling constant  ${}^2J_{\text{PP}}$  of 144 Hz, as expected for complexes with two magnetically different phosphorus atoms in the metal coordination sphere. Free  $\text{P}(\text{pyr})_3$  resonates at 78.8 ppm in the  ${}^{31}\text{P}\{^1\text{H}\}$  NMR spectrum, and the chemical shifts for the complex indicate coordination of the ligand. The complex  $[\text{RuCl}(\text{ind})\{\text{P}(\text{pyr})_3\}_2]$  exhibited only one signal in the  ${}^{31}\text{P}\{^1\text{H}\}$  NMR spectrum at 122.2 ppm, as expected for two identical phosphorus atoms coordinated to the ruthenium center.

The indenyl ligand gives very distinct  ${}^1\text{H}$  and  ${}^{13}\text{C}\{^1\text{H}\}$  NMR signals for the three protons and the five carbon atoms of its coordinated five-membered ring.<sup>[23]</sup> Due to the unsymmetrical substitution pattern with four different ligands in  $[\text{RuCl}(\text{ind})(\text{PPh}_3)\{\text{P}(\text{pyr})_3\}]$ , all these carbons and protons are diastereotopic and give individual signals in the corresponding NMR spectra. In  $[\text{RuCl}(\text{ind})\{\text{P}(\text{pyr})_3\}_2]$ , the complex is symmetric, due to the two  $\text{P}(\text{pyr})_3$  ligands, and chemically equivalent protons and carbon atoms give only one set of signals for the cyclopentadienyl portion of the complex, simplifying the  ${}^1\text{H}$  and  ${}^{13}\text{C}\{^1\text{H}\}$  NMR spectrum.

### **X-Ray structures**

In order to unequivocally establish the structure of the new ruthenium complexes, the X-ray structure of the complexes  $[\text{RuCl}(\text{ind})(\text{PPh}_3)\{\text{P}(\text{pyr})_3\}]$  and  $[\text{RuCl}(\text{ind})\{\text{P}(\text{pyr})_3\}_2]$  were determined (Tables 1 and Figure 2). Selected bond lengths and angles are listed in Table 2, and for comparison purposes, the X-Ray data for  $[\text{RuCl}(\text{ind})(\text{PPh}_3)_2]$  taken from the literature are also included.<sup>[24]</sup>



The bond angles for the monodentate ligands about the ruthenium center range from  $89.510(13)^\circ$  to  $99.008(14)^\circ$ . The structures are, thus, best described as a slightly distorted octahedral. The greatest deviation from this ideal  $90^\circ$  angle are for both complexes the P(1)-Ru-P(2) angles [ $97.89(5)^\circ$  and  $99.008(14)^\circ$ ], suggesting some steric repulsion between  $\text{PPh}_3$  and  $\text{P}(\text{pyr})_3$  and between the two  $\text{P}(\text{pyr})_3$  ligands, respectively. Interestingly, the P(1)-Ru-P(2) angles for both complexes are comparable, which demonstrates that the  $\text{P}(\text{pyr})_3$  and the  $\text{PPh}_3$  ligands have similar steric demand.

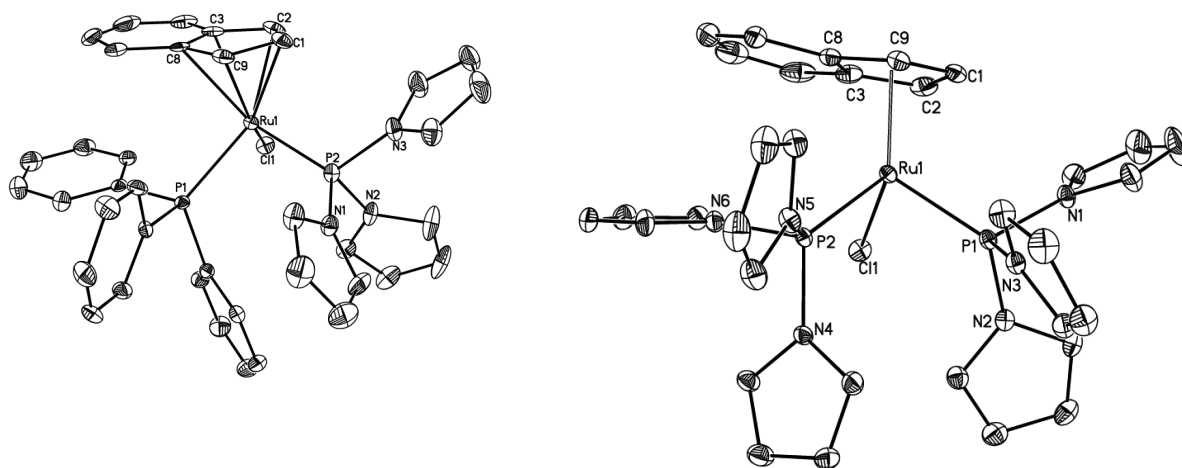


**Figure 2.** The molecular structures of  $[\text{RuCl}(\text{ind})(\text{PPh}_3)\{\text{P}(\text{pyr})_3\}]$  (left) and  $[\text{RuCl}(\text{ind})\{\text{P}(\text{pyr})_3\}_2]$ . Hydrogen atoms are omitted for clarity. Crystallographic parameters are compiled in Table 1, and key bond lengths and angles are listed in Table 2.

**Table 1.** Crystallographic Parameters

	[RuCl(ind)(PPh <sub>3</sub> ){P(pyr) <sub>3</sub> } <sub>2</sub> ]	[RuCl(ind){P(pyr) <sub>3</sub> } <sub>2</sub> ]	Xanthenone <b>7b</b>
Empirical formula	C <sub>39</sub> H <sub>34</sub> ClN <sub>3</sub> P <sub>2</sub> Ru	C <sub>33</sub> H <sub>31</sub> ClN <sub>6</sub> P <sub>2</sub> Ru	C <sub>27</sub> H <sub>24</sub> O <sub>3</sub>
Formula weight	743.15	710.10	396.46
Temperature K / Wavelength Å	100(2) / 0.71073	100(2) / 0.71073	100(2) K / 0.71073Å
Crystal system	Orthorhombic	Monoclinic	Triclinic
Space group	P <sub>bca</sub>	P2 <sub>1</sub> /c	P $\bar{1}$
Unit cell dimensions	a = 17.9518(15) Å b = 15.6316(12) Å c = 24.057(2) Å $\alpha = 90^\circ$ $\beta = 90^\circ$ $\gamma = 90^\circ$	a = 13.2598(6) Å b = 9.5844(4) Å c = 24.8271(11) Å $\alpha = 90^\circ$ $\beta = 99.205(2)^\circ$ $\gamma = 90^\circ$	a = 10.1854(6) Å b = 12.5276(7) Å c = 17.3162(9) Å $\alpha = 105.980(3)^\circ$ $\beta = 92.278(3)^\circ$ $\gamma = 107.377(3)^\circ$
Volume / Z	6750.8(9) Å <sup>3</sup> / 8	3114.6(2) Å <sup>3</sup> / 4	2009.2(2) Å <sup>3</sup> / 4
Density (calculated)	1.462 Mg/m <sup>3</sup>	1.514 Mg/m <sup>3</sup>	1.311 Mg/m <sup>3</sup>
Absorption coefficient	0.672 mm <sup>-1</sup>	0.726 mm <sup>-1</sup>	0.084 mm <sup>-1</sup>
F(000)	3040	1448	840
Crystal size / mm <sup>3</sup>	0.346 x 0.235 x 0.076	0.256 x 0.151 x 0.135	0.298 x 0.275 x 0.243
Theta range for data collection	1.924 to 27.161°	1.556 to 36.325°	1.234 to 30.571°
Index ranges	-21 ≤ h ≤ 23, -20 ≤ k ≤ 15, -30 ≤ l ≤ 27	-22 ≤ h ≤ 22, -15 ≤ k ≤ 14, -41 ≤ l ≤ 41	-12 ≤ h ≤ 14, -17 ≤ k ≤ 17, -24 ≤ l ≤ 24
Reflections collected	78357	69845	48129
Independent reflections	7471 [R(int) = 0.0733]	15058 [R(int) = 0.0603]	12106 [R(int) = 0.0413]
Absorption correction	Semi-empirical from equivalents	Semi-empirical from equivalents	Semi-empirical from equivalents
Max. and min. transmission	0.7989 and 0.7989	0.8625 and 0.7561	0.8879 and 0.8189
Data / restraints / parameters	7471 / 1 / 415	15058 / 0 / 388	12106 / 1 / 541
Goodness-of-fit on F <sup>2</sup>	1.003	1.019	1.028
Final R indices [I > 2σ(I)]	R1 = 0.0319, wR2 = 0.0604	R1 = 0.0361, wR2 = 0.0745	R1 = 0.0525, wR2 = 0.1314
R indices (all data)	R1 = 0.0596, wR2 = 0.0706	R1 = 0.0559, wR2 = 0.0831	R1 = 0.0892, wR2 = 0.1546
Largest diff. peak and hole / e.Å <sup>-3</sup>	0.479 and -0.511	0.759 and -0.683	0.365 and -0.324

**Table 2.** Selected bond lengths and angles

	[RuCl(Ind)(PPh <sub>3</sub> ){P(pyr) <sub>3</sub> }]	[RuCl(Ind){P(pyr) <sub>3</sub> } <sub>2</sub> ]	[RuCl(Ind)(PPh <sub>3</sub> ) <sub>2</sub> ]
<i>Bond lengths (Å)</i>			
Ru-P(1)	2.2323(15) (P(Pyr) <sub>3</sub> )	2.2042(4)	2.331
Ru-P(2)	2.2760(14) (PPh <sub>3</sub> )	2.2716(4)	2.268
Ru-Cl	2.4362(15)	2.4251(4)	2.437
P(1)-N(X) <sup>a</sup> average	1.712	1.716	-
P(1)-C(X) <sup>a</sup> average	1.831	-	-
<i>Bond Angles (°)</i>			
P(1)-Ru-P(2)	97.89(5)	99.008(14)	99.21
Cl-Ru-P(1)	93.51(5)	90.684(14)	92.42
Cl-Ru-P(2)	91.79(5)	89.510(13)	92.19
<i>Other geometrical parameters</i>			
Ru-Cp (Å) <sup>b</sup>	1.902	1.928	1.918
Δ Ru-C <sup>c</sup>	0.161	0.155	0.221
Fold angle <sup>d</sup>	7.06°	7.33	7.07

<sup>a</sup> P(1)-N(X) corresponds to the P-N bonds of P(pyr)<sub>3</sub>. P(1)-C(X) corresponds to the P-C bonds of PPh<sub>3</sub>

<sup>b</sup> Distance between the Cp-centroid of the indenyl ligand and the ruthenium center.

<sup>c</sup> Average difference between the Ru-C1, Ru-C2 and Ru-C9 bond lengths and the Ru-C3 and Ru-C8 bond lengths, see Figure 3.

<sup>d</sup> Angle between the plane formed by C1-C2-C9 and by C2-C3-C8-C9, see Figure 3.

The Ru–P bond length for the P(pyr)<sub>3</sub> ligand in [RuCl(ind)(PPh<sub>3</sub>){P(pyr)<sub>3</sub>}] [2.2323(15) Å] is only slightly shorter than that found for the PPh<sub>3</sub> ligand [2.2760(14) Å], which might be due to increased backbonding from the ruthenium to the P(pyr)<sub>3</sub> ligand.<sup>[11,13a]</sup> Furthermore, in [RuCl(ind){P(pyr)<sub>3</sub>}<sub>2</sub>], the Ru–P bond length for both P(pyr)<sub>3</sub> ligands are also slightly different [2.2042(4) and 2.2716(4) Å, respectively], but fall in the range of other ruthenium P(pyr)<sub>3</sub> complexes.<sup>[11,14e]</sup> Also, the distance between the Cp-centroid of the indenyl ligand and the ruthenium center for both complexes are similar to each other (1.902 and 1.928 Å) and comparable to that found for [RuCl(ind)(PPh<sub>3</sub>)<sub>2</sub>] (1.918 Å). Thus, the angles and the bond lengths for the P(pyr)<sub>3</sub> ligand are comparable to the PPh<sub>3</sub> ligand and overall, the geometric parameters for the two P(pyr)<sub>3</sub> complexes and [RuCl(ind)(PPh<sub>3</sub>)<sub>2</sub>] are similar, and the Ru–P(pyr)<sub>3</sub> bond lengths are at best slightly shorter than the Ru–P(pyr)<sub>3</sub> bond lengths.

The P–N bond lengths of the P(pyr)<sub>3</sub> ligand (1.712 and 1.716 Å) are slightly longer than the typical P–N bond lengths of phosphoramidite ligands R<sub>2</sub>NP(OR)<sub>2</sub> (around 1.66 Å), suggesting a substantial P=N double bond character in the phosphoramidite ligand.<sup>[13a,14a]</sup> The elongated P–N bond lengths in the P(pyr)<sub>3</sub> ligand are in accordance with aromatic delocalization of the nitrogen lone pair into the five-membered pyrrolyl ring as previously described,<sup>[9]</sup> preventing formation of a double bond with the phosphorus.

As can be seen from the X-Ray structures, the indenyl ligands for both complexes are η<sup>5</sup>-coordinated, i.e. all five carbon atoms of the cyclopentadienyl unit form bonds to the ruthenium center. However, it has been described previously that the Ru–C bond lengths for

the coordinated cyclopentadienyl unit are not all of the same lengths as is the case for the two complexes described herein. As, with some exaggeration, illustrated in Figure 3 (top left), the cyclopentadienyl unit in indenyl complexes is typically slipped in a way that the bond lengths of the two benzenoid carbons are longer than the bond lengths to the other three carbon atoms. This has been ascribed to a gain in resonance energy for the aryl ring of the ligand.<sup>[21e]</sup> In an extreme case, only three of the five carbons would bond to the ruthenium center in an  $\eta^3$ -fashion (Figure 3, top right).<sup>[21e]</sup> The degree of the slippage has previously been quantified by two parameters taken from X-Ray data, the  $\Delta M-C$  value and the fold angle.<sup>[21e,25]</sup> The  $\Delta M-C$  value is the average difference between the Ru-C1, Ru-C2 and Ru-C9 bond lengths and the Ru-C3 and Ru-C8 bond lengths in the structures in Figure 2. Ideally, it is 0 and values around 0.2 Å are typical for indenyl ligands, indicating  $\eta^5$ -coordination. The values for  $[\text{RuCl}(\text{ind})(\text{PPh}_3)\{\text{P}(\text{pyr})_3\}]$  and  $[\text{RuCl}(\text{ind})\{\text{P}(\text{pyr})_3\}_2]$  fall in this range. The fold angle is the angle between the plane formed by C1-C2-C8 and by C2-C3-C8-C9 (Figure 3, top right); it takes the value 0 in an ideal  $\eta^5$ -coordination, and for indenyl complexes, the values typically range below 10°; again,  $[\text{RuCl}(\text{ind})(\text{PPh}_3)\{\text{P}(\text{pyr})_3\}]$  and  $[\text{RuCl}(\text{ind})\{\text{P}(\text{pyr})_3\}_2]$  fall in this range. An  $\eta^3$ -coordination would be indicated by a fold angle around 60°.<sup>[21e]</sup>

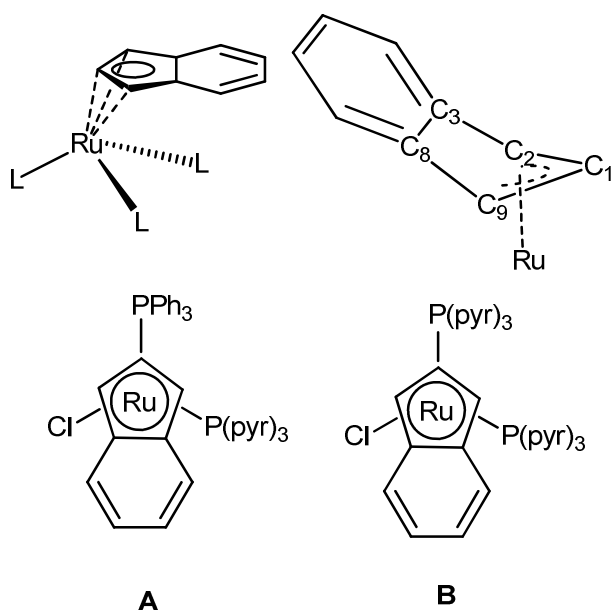


**Figure 3.** Geometric parameters for indenyl complexes.

However, what is interesting for the two complexes is which ligand takes the position *trans* to the C<sub>3</sub> and C<sub>8</sub> benzo-carbons of the cyclopentadienyl unit. It has been demonstrated before that the ligand with the strongest *trans* influence will take the position *trans* to the benzo unit, weakening the bond strength (and enlarging the bond length) of the two Ru-C bonds of the benzo unit.<sup>[21e]</sup> In [RuCl(ind){P(pyr)<sub>3</sub>}<sub>2</sub>], one of the two P(pyr)<sub>3</sub> ligands is located *trans* to the benzo-ring, indicating that P(pyr)<sub>3</sub> has a stronger *trans* influence than chloride (**B** in Figure 3, bottom). However, in [RuCl(ind)(PPh<sub>3</sub>){P(pyr)<sub>3</sub>}], the PPh<sub>3</sub> ring is located in the *trans* position (**A** in Figure 3, bottom), indicating that PPh<sub>3</sub> has a stronger *trans* influence than P(pyr)<sub>3</sub>. This observation might be ascribed to the higher  $\sigma$ -basicity of PPh<sub>3</sub> compared to P(pyr)<sub>3</sub>, which leads to a stronger *trans*-influence.

The basicity of ligands has in the past been assessed through the  $\nu_{\text{CO}}$  stretching frequencies of carbonyl complexes, and indeed, the value for  $\text{P}(\text{pyr})_3$  is higher ( $2024 \text{ cm}^{-1}$ ) than for  $\text{PPh}_3$  ( $1980 \text{ cm}^{-1}$ ) in *trans*- $[\text{RhCl}(\text{CO})\text{L}_2]$  ( $\text{L} = \text{P}(\text{pyr})_3, \text{PPh}_3$ ) indicating higher basicity of the latter.<sup>[9]</sup> Further evidence for the higher basicity of  $\text{PPh}_3$  compared to  $\text{P}(\text{pyr})_3$  are  $^{31}\text{P}$ - $^{77}\text{Se}$  coupling constants, which increase with decreasing basicity of the phosphorus compound.<sup>[26]</sup> In accordance with the higher basicity of  $\text{PPh}_3$ ,  $\text{Se}=\text{P}(\text{pyr})_3$  exhibits a  $J_{\text{P-Se}}$  value around 970 Hz, which is significantly higher than the corresponding value for  $\text{Se}=\text{PPh}_3$  (735 Hz).<sup>[27]</sup>

### Cyclic Voltammetry

Overall, the solid state structures of  $[\text{RuCl}(\text{ind})(\text{PPh}_3)\{\text{P}(\text{pyr})_3\}]$  and  $[\text{RuCl}(\text{ind})\{\text{P}(\text{pyr})_3\}_2]$  revealed some similarities between these two complexes and  $[\text{RuCl}(\text{ind})(\text{PPh}_3)_2]$ . The structural parameters around the ruthenium center are comparable, corroborating earlier statements that the  $\text{PPh}_3$  and  $\text{P}(\text{pyr})_3$  ligands are sterically similar. Electronic differences could be observed through the stronger trans influence of  $\text{PPh}_3$  compared to  $\text{P}(\text{pyr})_3$  and through the higher  $J_{\text{P-Se}}$  coupling constants in  $\text{Se}=\text{P}(\text{pyr})_3$ . Cyclic voltammetry has been used before to characterize the electronic properties of ruthenium phosphine complexes.<sup>[28]</sup> To obtain further insight into the electronic properties of the new complexes, cyclic voltammograms were recorded of  $[\text{RuCl}(\text{ind})(\text{PPh}_3)\{\text{P}(\text{pyr})_3\}]$  and  $[\text{RuCl}(\text{ind})\{\text{P}(\text{pyr})_3\}_2]$ , and also, for comparison, of  $[\text{RuCl}(\text{ind})(\text{PPh}_3)_2]$ . The traces for a scan rate of 0.8 V/s are compiled in Figure 4.

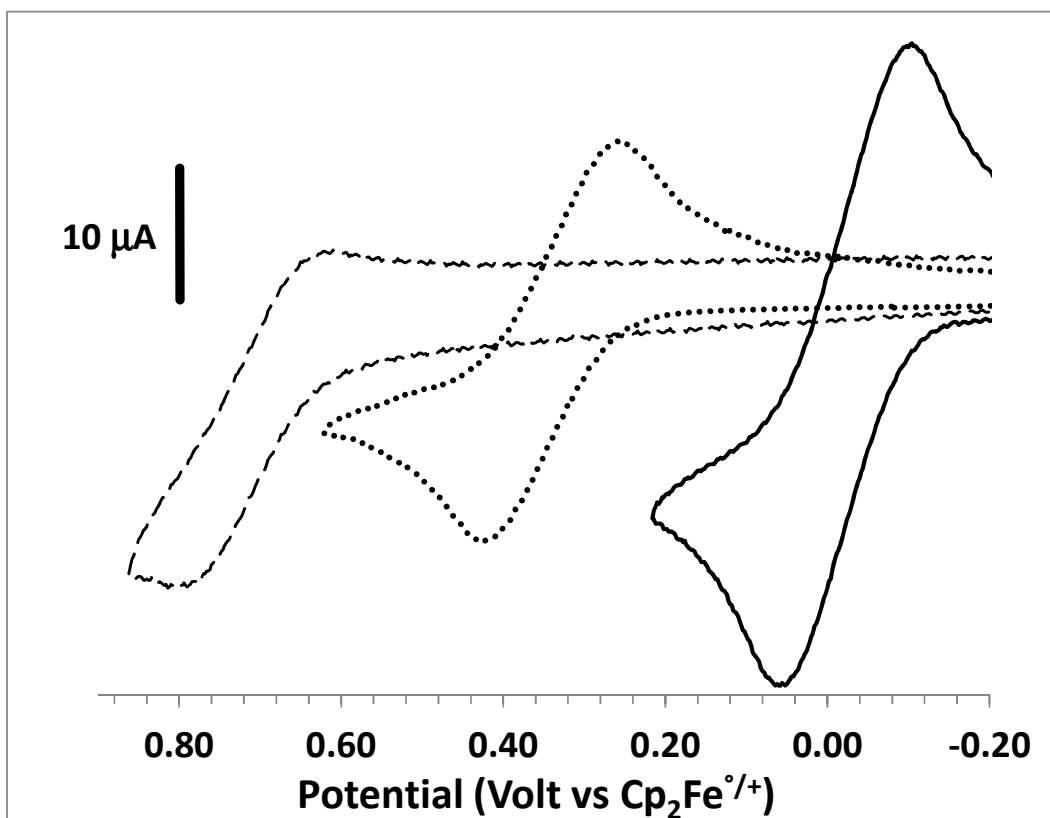


**Figure 4.** Cyclic voltammometry of ruthenium indenyl complexes in 0.1M  $\text{Bu}_4\text{PF}_6 / \text{CH}_2\text{Cl}_2$ , 298K, recorded at a scan rate of 0.8 V/s.  $[\text{RuCl}(\text{ind})(\text{PPh}_3)_2]$  (solid line),  $[\text{RuCl}(\text{ind})(\text{PPh}_3)\{\text{P}(\text{pyr})_3\}]$  (dotted line  $\cdots$ ),  $[\text{RuCl}(\text{ind})\{\text{P}(\text{pyr})_3\}_2]$  (dashed line  $---$ ).

The cyclic voltammogram of  $[\text{RuCl}(\text{ind})(\text{PPh}_3)_2]$  shows a high degree of reversibility at different scan rates in that its  $i_{pc}/i_{pa}$  values are close to a value of 1 at all scan rates. The  $E^{\circ'}$  value for the oxidation is  $-0.023 \text{ V}$  (vs.  $\text{Cp}_2\text{Fe}^{0/+}$ , Cp = cyclopentadienyl) and the peak current ratio  $i_{pc}/i_{pa}$  is 1.0 at a scan rate of 0.8 V/s. For the complexes  $[\text{RuCl}(\text{ind})(\text{PPh}_3)\{\text{P}(\text{pyr})_3\}]$  and  $[\text{RuCl}(\text{ind})\{\text{P}(\text{pyr})_3\}_2]$ , the  $E^{\circ'}$  values are significantly higher ( $+0.34$  and  $+0.71 \text{ V}$ , respectively). The oxidation of  $[\text{RuCl}(\text{ind})(\text{PPh}_3)\{\text{P}(\text{pyr})_3\}]$  is



still reversible at different scan rates with an  $i_{pc}/i_{pa}$  ratio of 1.0 at 0.8 V/s. However, the oxidation of  $[\text{RuCl}(\text{ind})\{\text{P}(\text{pyr})_3\}_2]$  only shows some reversibility at high scan rates of 0.8 V/s and 1.6 V/s, with low  $i_{pc}/i_{pa}$  ratios of 0.7 to 0.8, respectively, indicating decomposition of the oxidized species. It appears that the successive introduction of  $\text{P}(\text{pyr})_3$  ligands increases the oxidation potential of the respective complexes, which is in line with the higher  $\pi$ -acidic electron-demand of that ligand. The presence of two  $\text{P}(\text{pyr})_3$  ligands in  $[\text{RuCl}(\text{ind})\{\text{P}(\text{pyr})_3\}_2]$  destabilize the oxidized species  $[\text{RuCl}(\text{ind})\{\text{P}(\text{pyr})_3\}_2]^+$  as can be seen from the decreased reversibility of the oxidative cyclic voltammogram waves, suggesting some decomposition after oxidation, possibly by attack of adventitious nucleophiles.

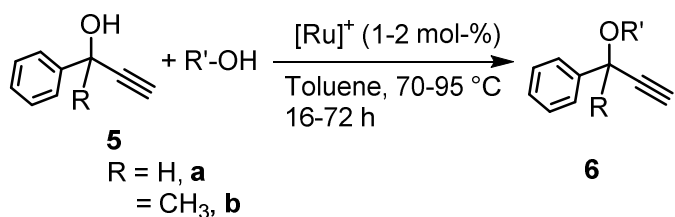
Overall, the combined X-Ray, NMR and CV data demonstrate that the  $\text{P}(\text{pyr})_3$  ligand shows  $\pi$ -acidic behaviour and it is a weaker  $\sigma$  donor compared to  $\text{PPh}_3$ . However, sterically, the  $\text{P}(\text{pyr})_3$  ligand resembles  $\text{PPh}_3$ , as can be seen from the comparable bond lengths and angles for both of them around the ruthenium center. It appears that the tris-*N*-pyrrolyl phosphine has steric properties similar to  $\text{PPh}_3$ , despite its profound impact on the electron density at the metal. Consequently, tris-*N*-pyrrolyl phosphine can be utilized in the synthesis of complexes with decreased electron density at the metal but steric properties similar to their respective  $\text{PPh}_3$  derivatives.

### **Catalytic applications**

We then investigated the new complexes in their ability to catalytically activate propargylic alcohols,<sup>[29]</sup> and we chose the etherification of propargylic alcohols **5** as a test

reaction (Table 3).<sup>[15a,c]</sup> The complexes  $[\text{RuCl}(\text{ind})(\text{PPh}_3)\{\text{P}(\text{pyr})_3\}]$  and  $[\text{RuCl}(\text{ind})\{\text{P}(\text{pyr})_3\}_2]$  themselves did not show catalytic activity for the reaction. However, after activation through chloride abstraction using  $\text{Et}_3\text{OPF}_6$ , we observed catalytic activity. After some optimization efforts, we found that 1-2 mol-% of activated  $[\text{RuCl}(\text{ind})(\text{PPh}_3)\{\text{P}(\text{pyr})_3\}]$  catalyzed the etherification of a number of propargylic alcohols **5** to give the corresponding propargyl ethers **6** in 42 to 27% isolated yields (toluene solvent, 70 to 95 °C for 16-72 h). The complex  $[\text{RuCl}(\text{ind})\{\text{P}(\text{pyr})_3\}_2]$  showed no catalytic activity for the etherification reactions in Table 3, even after activation through chloride abstraction. We do currently not have a satisfactory explanation for the different catalytic activities of the two complexes in the etherification reactions; it is possible that the alcohol substrates for the etherification reaction deactivate the catalytically active species derived from  $[\text{RuCl}(\text{ind})\{\text{P}(\text{pyr})_3\}_2]$ .

Excess of the alcohol nucleophile over the propargylic alcohol is not required and the catalyst load of 1-2 mol-% is lower than that of other catalyst systems.<sup>[14]</sup> Some catalytic systems reported in the literature perform the etherification reactions in Table 3 using the alcohol nucleophile as the solvent.<sup>[14]</sup> We speculated that the yields could be improved by running the reaction in neat alcohols as the solvent and did so for the entries 3 and 4 of Table 3. In neat *n*-butanol, only trace quantities of the product were observed and in neat benzylic alcohol, conversion to the product was detected by GC, but starting material **5b** was still present in the reaction mixture. Thus, the reaction is not more efficient utilizing the alcohol nucleophiles as the solvent, which we tentatively ascribe to the deactivation of the catalyst by the alcohols.

**Table 3.** Isolated Yields.

Entry <sup>a</sup>	Substrates	Product	Yield / %
1			38 <sup>b</sup>
2			37 <sup>b</sup>
3			42 <sup>c</sup>
4			41 <sup>d</sup>
5			27 <sup>c</sup>

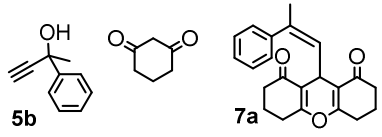
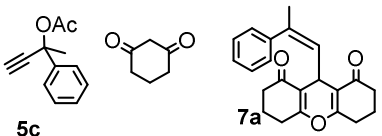
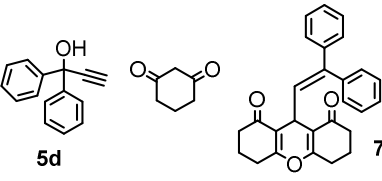
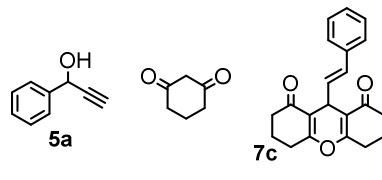
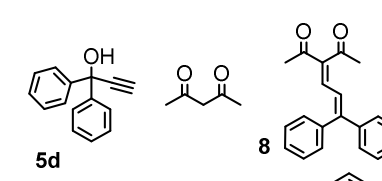
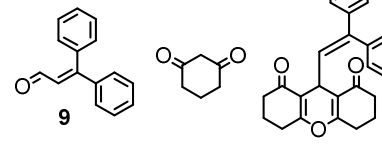
<sup>a</sup> General conditions: Propargylic alcohol (0.7 mmol) and alcohol R'-OH (1 mmol) in toluene (2 mL) catalyzed by activated [RuCl(Indenyl)(PPh<sub>3</sub>){P(pyr)<sub>3</sub>}] (0.007 mmol). The products were isolated chromatographically.

<sup>b</sup> 70 °C for 16 hr. <sup>c</sup> 85 °C for 18 hr. <sup>d</sup> 95 °C for 72 hr.

We then turned over to carbon centered nucleophiles in the form of diketones (Table 4), which have previously been utilized for the substitution of the OH unit of propargylic alcohols.<sup>[14,29d,e]</sup> When subjected to the same reaction conditions as in Table 3, we did not observe the formation of the corresponding substitution products. Instead, we detected

xanthenone derivatives **7** in the crude reaction mixtures when cyclohexane-1,3-dione was used as the diketone substrate. Again, after some optimization efforts, we determined that the ruthenium complexes  $[\text{RuCl}(\text{ind})(\text{PPh}_3)\{\text{P}(\text{pyr})_3\}]$  and  $[\text{RuCl}(\text{ind})\{\text{P}(\text{pyr})_3\}_2]$ , after activation through chloride abstraction, catalyzed the synthesis of the xanthenone derivatives **7a-c** from propargylic alcohols and 2 equivalents of cyclohexane-1,3-dione (80 to 95 °C, 72 h, 67-22 % isolated yields, Table 4). For propargylic alcohol **5b**, we found that the corresponding propargylic acetate **5c** gave higher yields (Table 4, entry 2). The higher yields might be explained through the fact that the acetate group is a better leaving group than OH. Furthermore, it has been reported in the literature that carboxylic acids<sup>[30]</sup> or trifluoro acetic acid<sup>[16j,k]</sup> have a beneficial effect on ruthenium catalyzed isomerization reactions. The acetate leaving group might convert to acetic acid after departure, making the catalyst system - in line with these literature reports - more efficient. The identity of the xanthenones **7** was established through X-Ray analysis of product **7b** in Table 4 (Figure 5). For the product **7a**, *E* and *Z* isomers can form during catalysis, and we determined by <sup>1</sup>H NMR an *Z* / *E* ratio of 4.1:1 and 8:1 for the transformation of **5b** and **5c**, respectively. We tentatively assigned the *Z* configuration to the major isomer of this compound by analogy to a closely related trisubstituted alkene.<sup>[31]</sup> Product **7c** is known<sup>[32]</sup> and was isolated as the pure *E* isomer, as determined by NMR and comparison of the chemical shifts with the literature values. The high reaction temperatures and somewhat elongated reaction times might promote the formation of the thermodynamically more stable *E* isomer. The xanthenones **7a** and **b** in Table 4 are new and xanthene derivatives are known to exhibit pharmaceutical activity.<sup>[33]</sup>

**Table 4.** Isolated Yields

Entry	Substrates	Product
1 <sup>a</sup>		22% <sup>b</sup> 34% <sup>c</sup>
2 <sup>a</sup>		46% <sup>b</sup> 67% <sup>c</sup>
3 <sup>a</sup>		69% <sup>c</sup>
4 <sup>d</sup>		29% <sup>c</sup>
5 <sup>e</sup>		34% <sup>b</sup> 40% <sup>c</sup>
6 <sup>f</sup>		32% <sup>c</sup>

<sup>a</sup> Conditions: 2.5 mol equivalents dione, in ClCH<sub>2</sub>CH<sub>2</sub>Cl (2 mL) for 72 hours at 80-95 °C. The products were isolated chromatographically.

<sup>b</sup> Catalyst 1-2 mol-% [Ru(Indenyl){P(pyr)<sub>3</sub>}<sub>2</sub>]<sup>+</sup>.

<sup>c</sup> Catalyst 1-2 mol-% [Ru(Indenyl)(PPh<sub>3</sub>){P(pyr)<sub>3</sub>}]<sup>+</sup>.

<sup>d</sup> Conditions: 2.5 mol equivalents dione, in cyclohexane (2 mL) for 16 hours at 90 °C. The products were isolated chromatographically.

<sup>e</sup> Conditions: 2.5 mol equivalents dione, in Cl<sub>2</sub>CH<sub>2</sub>CH<sub>2</sub>Cl (2 mL) for 18-48 hours at 85-90 °C. The products were isolated chromatographically.

<sup>f</sup> Conditions: 2.5 mol equivalents dione, in ClCH<sub>2</sub>CH<sub>2</sub>Cl (2 mL) for 18 hours at 85 °C. 4 mol-% catalyst loading. The product was isolated chromatographically.

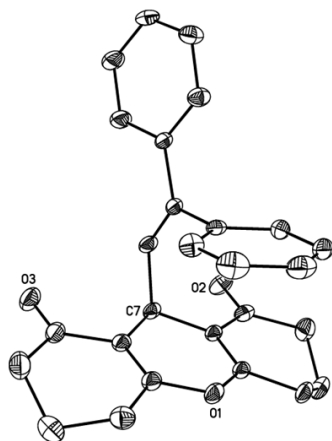


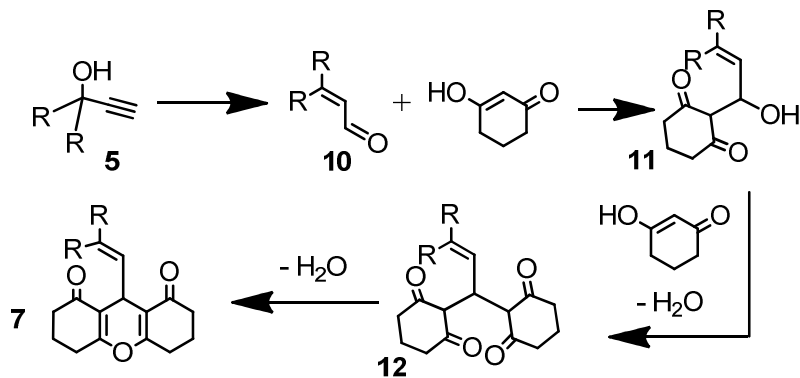
**Figure 5.** Molecular structure of xanthenone **7b**.

When pentane-2,4-dione was used as the diketone (Table 4, entry 5), a related reaction took place where the diketone condensed with the rearranged propargylic alcohol to give the known conjugated allylidene dione **8**, which has previously been synthesized utilizing catalytic *p*-toluenesulfonic acid under reflux conditions.<sup>[34]</sup>

In contrast to the etherification reactions in Table 3, it seemed that activated  $[\text{RuCl}(\text{ind})(\text{PPh}_3)\{\text{P}(\text{pyr})_3\}]$  and  $[\text{RuCl}(\text{ind})\{\text{P}(\text{pyr})_3\}_2]$  gave comparable yields in the chemistry of Table 4.

Although the exact mechanism of the reactions remains to be investigated, they can be viewed as a tandem isomerization / condensation sequence (Scheme 2).<sup>[35,36]</sup> Propargylic alcohols are known to undergo acid catalyzed Meyer-Schuster rearrangements to their corresponding aldehydes **9** (Scheme 2).<sup>[14,37]</sup> The aldehydes formed from the propargylic alcohols in Table 4 can then undergo a double aldol condensation with the enol tautomer of the dione followed by a hemi-acetal formation / dehydration sequence as suggested by

others.<sup>[35,36]</sup> Indeed, when 3,3-diphenylacrylaldehyde **9** was utilized in the reaction with cyclohexane-1,3-dione, the product **7b** was isolated in a somewhat lower yield of 32% (Table 4, entry 6), suggesting that the aldehyde might be an intermediate for the reaction.



**Scheme 2.** Tandem isomerization - aldol sequence to give xanthenones **7**.

The formation of xanthenones from aldehydes and diketones is, in principle, known, and has been reported to be catalyzed by Brønsted<sup>[38]</sup> or Lewis acids,<sup>[35,39]</sup> catalyst free<sup>[36]</sup> or by iodine.<sup>[40]</sup> However, to the best of our knowledge, the chemistry in Table 4 and Scheme 2 represents the first example of the ruthenium catalyzed conversion of propargylic alcohols (not aldehydes) to xanthenones, and the first ruthenium catalyzed version of the reaction. A gold catalyzed conversion of propargylic alcohols to xanthenones has previously been described in the literature.<sup>[41]</sup> Further investigations into the mechanism are currently underway.

## Conclusion

The synthesis of the first tris-*N*-pyrrolyl phosphine indenyl ruthenium complexes [RuCl(ind)(PPh<sub>3</sub>){P(pyr)<sub>3</sub>}] and [RuCl(ind){P(pyr)<sub>3</sub>}<sub>2</sub>] is described. As determined through

X-Ray analysis and cyclic voltammetry, the tris-*N*-pyrrolyl phosphine ligand is more  $\pi$ -acidic and less  $\sigma$  donating compared to PPh<sub>3</sub>. However, the steric properties of both ligands in the solid state are comparable, as can be seen from the bond lengths and angles associated with the ruthenium centers derived from X-Ray data. The new complexes are - after chloride abstraction - catalytically active in the etherification of propargylic alcohols and in a tandem isomerisation – condensation sequence to give xanthenones.

## Experimental

**General.** All reactions were carried out under an inert N<sub>2</sub> atmosphere using standard Schlenk techniques. All chemicals were used as supplied from Sigma-Aldrich unless otherwise noted. The complex [RuCl(ind)(PPh<sub>3</sub>)<sub>2</sub>] was synthesized following the literature.<sup>[18]</sup> THF was distilled from Na/benzophenone under N<sub>2</sub>. Ethyl acetate, hexane, toluene, CH<sub>2</sub>Cl<sub>2</sub>, and ClCH<sub>2</sub>CH<sub>2</sub>Cl were used as received. Pyrrole was vacuum distilled over CaCl<sub>2</sub> prior to use. All propargylic alcohols, alcohols, and ketones were obtained and used as provided from Sigma-Aldrich. 1-Phenyl-2-propyn-1-ol and propargyl acetate **5c** were synthesized according to literature procedures.<sup>[42,43]</sup>

NMR spectra for characterization were collected at room temperature on a Varian Unity 300 MHz or Bruker Avance 300 MHz instrument; all chemical shifts ( $\delta$ ) are reported in ppm and are referenced to a residual solvent signal. IR spectra were collected on a Thermo Nicolet 360 FT-IR spectrometer. FAB and exact mass data were collected on a JEOL MStation [JMS-700] Mass Spectrometer. Melting points were determined on a Thomas Hoover uni-



melt capillary melting point apparatus and are uncorrected. Elemental analyses were performed by Atlantic Microlab Inc., Norcross, GA, USA.

**[RuCl(ind)(PPh<sub>3</sub>){P(pyr)<sub>3</sub>}]**. A Schlenk flask containing [RuCl(ind)(PPh<sub>3</sub>)<sub>2</sub>] (0.658 g, 0.848 mmol), P(pyr)<sub>3</sub> (0.214 g, 0.932 mmol), and THF (8 mL) was refluxed gently for 4 hours under nitrogen. The solvent was removed via vacuum. The complex was isolated as a red solid (0.462 g, 0.622 mmol, 73%) by column chromatography (silica gel 2×15 cm, CH<sub>2</sub>Cl<sub>2</sub> as eluent), m.p. 120-122 °C (dec., capillary).

<sup>1</sup>H NMR (300 MHz, CDCl<sub>3</sub>) δ 7.51-7.45 (m, 6H, arom.), 7.33-7.13 (m, 13H, arom.), 6.14 (br s, 6H), 6.03 (br s, 6H), 4.86 (s, 1H, indenyl), 4.75 (s, 1H, indenyl), 4.54 (s, 1H, indenyl). <sup>13</sup>C{<sup>1</sup>H} NMR (75 MHz, CDCl<sub>3</sub>) δ 136.9 (d, *J*<sub>CP</sub>=42.6 Hz), 133.5 (d, *J*<sub>CP</sub>=10 Hz), 129.8 (s), 129.6 (s), 129.5 (s), 128.2 (d, *J*<sub>CP</sub>=9.5 Hz), 124.9 (s), 124.4 (s), 124.2 (d, *J*<sub>CP</sub>=6 Hz), 114.8 (s), 114.7 (s), 111.2 (d, *J*<sub>CP</sub>=6.5 Hz), 93.9 (s), 70.5 (d, *J*<sub>CP</sub>=7.5 Hz), 68.3 (d, *J*<sub>CP</sub>=6.0 Hz). <sup>31</sup>P{<sup>1</sup>H} NMR (121 MHz, CDCl<sub>3</sub>) δ 122.81 (d, *J*<sub>PP</sub>=144 Hz), 40.37 (d, *J*<sub>PP</sub>=144 Hz). IR (neat, solid):  $\tilde{\nu}$  = 3133 (w), 3052 (w), 2962 (w), 2359 (w), 1454 (m), 1437 (m), 1287 (w), 1178 (s), 1056 (s), 1036 (s), 732 (s), 696 (m), 623 (m) cm<sup>-1</sup>. HRMS: calcd. for C<sub>39</sub>H<sub>34</sub>N<sub>3</sub>P<sub>2</sub><sup>102</sup>Ru 708.1249; found 708.1282, corresponds to [Ru(ind){P(pyr)<sub>3</sub>}]<sup>+</sup>. C<sub>39</sub>H<sub>34</sub>N<sub>3</sub>P<sub>2</sub>RuCl (743.09): calcd. C 63.03, H 4.61; found C 62.77, H 4.59.

**[RuCl(ind){P(pyr)<sub>3</sub>}]<sub>2</sub>**. A Schlenk flask containing [RuCl(ind)(PPh<sub>3</sub>){P(pyr)<sub>3</sub>}] (0.140 g, 0.188 mmol), P(pyr)<sub>3</sub> (0.086 g, 0.380 mmol), and THF (5 mL) was refluxed gently for 5 hours under nitrogen. The solvent was removed via vacuum. The complex was isolated as an

orange-yellow solid (0.083 g, 0.117 mmol, 62%) by column chromatography (silica gel 2×15 cm, CH<sub>2</sub>Cl<sub>2</sub> as eluent), m.p. 126-128 °C (dec., capillary).

<sup>1</sup>H NMR (300 MHz, CDCl<sub>3</sub>) δ 7.19-7.16 (m, 4H, arom.), 6.40 (d, *J*<sub>HH</sub>=1.8 Hz, 12H), 6.17 (d, *J*<sub>HH</sub>=1.8 Hz, 12H), 5.21 (br s, 2H, indenyl), 4.75 (br s, 1H, indenyl). <sup>13</sup>C{<sup>1</sup>H} NMR (75 MHz, CDCl<sub>3</sub>) δ 131.1 (s), 124.4 (s), 124.2 (s), 112.9 (s), 112.4 (s), 96.1 (s), 70.8 (s). <sup>31</sup>P{<sup>1</sup>H} NMR (121 MHz, CDCl<sub>3</sub>) δ 122.2 (s). IR (neat, solid):  $\tilde{\nu}$  = 3127 (w), 3106 (w), 1453 (m), 1176 (s), 1083 (m), 1055 (s), 1033 (s), 736 (s), 712 (s), 703 (m), 614 (m) cm<sup>-1</sup>. HRMS: calcd. for C<sub>33</sub>H<sub>31</sub>N<sub>6</sub>P<sub>2</sub><sup>102</sup>Ru 675.1138; found 675.1140, corresponds to [Ru(ind)(PPh<sub>3</sub>){P(pyr)<sub>3</sub>}]<sup>+</sup>. C<sub>33</sub>H<sub>31</sub>N<sub>6</sub>P<sub>2</sub>RuCl (710.08): calcd. C 55.82, H 4.40; found C 55.80, H 4.32.

#### **Activation of [RuCl(ind)(PPh<sub>3</sub>){P(pyr)<sub>3</sub>}] through chloride abstraction.**

[RuCl(ind)(PPh<sub>3</sub>){P(pyr)<sub>3</sub>}] was placed into a Schlenk tube, along with a molar equivalent of triethyloxonium hexafluorophosphate (Et<sub>3</sub>OPF<sub>6</sub>), and CH<sub>2</sub>Cl<sub>2</sub>. The mixture was stirred under N<sub>2</sub> for 2-4 hours, followed by removal of the solvent via vacuum to isolate the activated catalyst as a dark tan solid.

#### **Representative example for the catalysis reactions in Table 3.**

**(2-(benzyloxy)but-3-yn-2-yl)benzene.** From 2-phenyl-3-butyne-2-ol (**5b**, Table 3, entry 3). To a small screw-cap vial containing 2-phenyl-3-butyne-2-ol (**5b**, 0.105 g, 0.72 mmol), benzyl alcohol (0.154 g, 1.4 mmol) was added, along with toluene (2 mL). The activated catalyst was added (0.010 g, 0.007 mmol, 1 mol-%) and the mixture was heated at 100 °C for 72 hours. The product **6c** was isolated by column chromatography (silica gel, 1.5×15 cm, 2:1

hexane/CH<sub>2</sub>Cl<sub>2</sub>) as a dark yellow oil (0.071 g, 0.30 mmol, 42%). Spectroscopic data for all products in Table 3 are given in the Supporting Information and matched literature values.<sup>[15c]</sup>

#### Catalysis Reactions Table 4.

##### **(Z)-9-(2-phenylprop-1-en-1-yl)-3,4,5,6,7,9-hexahydro-1H-xanthene-1,8(2H)-dione**

**(7a)**. From propargyl alcohol **5b** (Table 4, entry 1). To a small screw-cap vial containing 2-phenyl-3-butyn-2-ol (**5b**, 0.138 g, 0.943 mmol), 1,3-cyclohexanedione (0.267 g, 2.381 mmol) was added, along with ClCH<sub>2</sub>CH<sub>2</sub>Cl (2 mL). The activated catalyst was added (0.010 g, 0.012 mmol, 1.3 mol-%) and mixture was heated at 80 °C for 72 hours. The product was isolated by column chromatography (silica gel, 1.5×15cm, 2:5 ethyl acetate/hexane) as an off-white solid (0.066 g, 0.197 mmol, 21%) as a 4.2:1 *Z* / *E* mixture of isomers as assessed by NMR. C<sub>22</sub>H<sub>22</sub>O<sub>3</sub> (334.16): calcd. C 79.02, H 6.63; found C 79.27, H 6.64. Major *Z* isomer: <sup>1</sup>H NMR (300 MHz, CDCl<sub>3</sub>) δ 7.53-7.09 (m, 5H, Ph), 5.17 (d, *J*<sub>HH</sub>=9.9 Hz, 1H), 4.62 (d, *J*<sub>HH</sub>=9.9 Hz, 1H), 2.45 (m, 11H), 1.97 (m, 4H); <sup>13</sup>C{<sup>1</sup>H} NMR (75 MHz, CDCl<sub>3</sub>) δ 196.7 (s), 164.5 (s), 144.1 (s), 136.3 (s), 128.7 (s), 128.1 (s), 126.7 (s), 126.1 (s), 116.1 (s), 37.2 (s), 27.4 (s), 26.2 (s), 20.6 (s), 16.3 (s).

Minor *E* isomer: <sup>1</sup>H NMR (300 MHz, CDCl<sub>3</sub>, partial) δ 5.56 (d, *J*<sub>HH</sub>=8.7 Hz), 4.24 (d, *J*<sub>HH</sub>=8.7 Hz); <sup>13</sup>C{<sup>1</sup>H} NMR (75 MHz, CDCl<sub>3</sub>) δ 163.9 (s), 142.6 (s), 138.0 (s), 128.3 (s), 127.9 (s), 127.3 (s), 126.4 (s), 116.5 (s), 42.3 (s), 38.3 (s), 37.1 (s), 27.8 (s), 27.2 (s), 26.3 (s), 21.9 (s), 20.3 (s).

From propargyl acetate **5c** (Table 4, entry 2). To a small screw-cap vial containing 2-phenyl-3-butyn-2-acetate (**5c**, 0.175 g, 0.934 mmol), 1,3-cyclohexanedione (0.265 g, 2.36 mmol) was added, along with ClCH<sub>2</sub>CH<sub>2</sub>Cl (2 mL). The activated catalyst was added (0.010 g, 0.012 mmol, 1.3 mol-%) and the mixture was heated at 80 °C for 72 hours. The product was isolated by column chromatography (silica gel, 1.5×15cm, 2:5 ethyl acetate/hexane) as an off-white solid (0.145 g, 0.435 mmol, 46%) as a 8:1 mixture of *Z* / *E* isomers as assessed by NMR. Spectroscopic data matched those reported above.

**9-(2,2-diphenylvinyl)-3,4,5,6,7,9-hexahydro-1H-xanthene-1,8(2H)-dione (7b)**. To a small screw-cap vial containing 1,1-diphenylprop-2-yn-1-ol (**5d**, 0.110 g, 0.528 mmol), 1,3-cyclohexanedione (0.212 g, 1.35 mmol) was added, along with ClCH<sub>2</sub>CH<sub>2</sub>Cl (2 mL). The activated catalyst was added (0.010 g, 0.014 mmol, 2.2 mol-%) and the mixture was heated at 85 °C for 72 hours. The product was isolated by column chromatography (silica gel, 1.5×15cm, 2:5 ethyl acetate/hexane) as an off-white solid (0.144 g, 0.363 mmol, 69%). <sup>1</sup>H NMR (300 MHz, CDCl<sub>3</sub>) δ 7.32-7.21 (m, 3H, Ph), 7.06-7.04 (m, 2H, Ph), 6.08 (d, *J*<sub>HH</sub>=9 Hz, 1H), 4.32 (d, *J*<sub>HH</sub>=9 Hz, 1H), 2.23 (m, 8H), 1.82 (m, 4H). <sup>13</sup>C{<sup>1</sup>H} NMR (75 MHz, CDCl<sub>3</sub>) δ 196.6 (s), 164.3 (s), 143.4 (s), 142.1 (s), 139.9 (s), 130.4 (s), 130.3 (s), 127.9 (s), 127.7 (s), 127.4 (s), 127.0 (s), 126.9 (s), 116.1 (s), 36.9 (s), 27.2 (s), 26.7 (s), 20.6(s). C<sub>27</sub>H<sub>24</sub>O<sub>3</sub> (396.48): calcd. C 81.79, H 6.10; found C 81.63, H 6.12.

**(E)-9-styryl-3,4,5,6,7,9-hexahydro-1H-xanthene-1,8(2H)-dione (7c)**.<sup>[32]</sup> To a small screw-cap vial containing 1-phenylprop-2-yn-1-ol (**5a**, 0.133 g, 1.01 mol), 1,3-

cyclohexanedione (0.292 g, 2.60 mmol) was added, along with cyclohexane (3 mL). The activated catalyst was added (0.016 g, 0.018 mmol, 1.8 mol-%) and mixture was heated at 90 °C for 16 hours. The product **7c** was isolated by column chromatography (silica gel, 1.5×15cm, 2:5 ethyl acetate/hexane) as an off-white solid (0.095 g, 0.296 mmol, 29%). <sup>1</sup>H NMR (300 MHz, CDCl<sub>3</sub>) δ 7.43-7.18 (m, 5H, Ph), 6.27 (s, 2H), 4.72 (s, 1H), 2.52 (m, 8H), 2.12 (m, 4H). <sup>13</sup>C{<sup>1</sup>H} NMR (75 MHz, CDCl<sub>3</sub>) δ 196.7 (s), 164.8 (s), 137.5 (s), 131.4 (s), 130.2 (s), 128.5 (s), 127.3 (s), 126.6 (s), 115.7 (s), 37.2 (s), 28.2 (s), 27.4 (s), 20.6 (s).

**3-(3,3-diphenylallylidene)pentane-2,4-dione (8)**. To a small screw-cap vial containing 1,1-diphenylprop-2-yn-1-ol (**5d**, 0.111 g, 0.532 mmol), 2,4-pentanedione (0.146 g, 1.45 mmol) was added, along with ClCH<sub>2</sub>CH<sub>2</sub>Cl (2 mL). The catalyst was added (0.010 g, 0.012 mmol, 2.4 mol-%) and mixture was heated at 85 °C for 16 hours. The product was isolated as tan oil by column chromatography (silica gel, 1.5×12cm, 2:5 ethyl acetate/hexane). The tan oil was dried via vacuum and dissolved into warm hexanes. Upon cooling, the product formed as an orange-white solid (0.054 g, 0.186 mmol, 34%). <sup>1</sup>H NMR (300 MHz, CDCl<sub>3</sub>) δ 7.53-7.46 (m, 4H, Ph), 7.41-7.32 (m, 4H, Ph), 7.32-7.25 (m, 2H, Ph), 7.19 (d, *J*<sub>HH</sub>=11.8 Hz, 1H), 7.07 (d, *J*<sub>HH</sub>=11.8 Hz, 1H), 2.46 (s, 3H, CH<sub>3</sub>), 2.20 (s, 3H, CH<sub>3</sub>'). <sup>13</sup>C{<sup>1</sup>H} NMR (75 MHz, CDCl<sub>3</sub>) δ 203.6 (s), 197.5 (s), 155.5 (s), 141.9 (s), 140.8 (s), 140.3 (s), 138.2 (s), 130.6 (s), 129.6 (s), 129.0 (s), 128.7 (s), 128.5 (s), 128.5 (s), 122.2 (s), 31.9 (s), 26.3 (s). C<sub>20</sub>H<sub>18</sub>O<sub>2</sub> (290.26): calcd. C 82.73, H 6.25; found C 82.28, H 6.24.

### Cyclic Voltammetry

Voltammograms were recorded in a three-electrode BAS electrochemical cell in a Vacuum Atmospheres HE-493 drybox under an atmosphere of argon in 0.1M  $\text{NBu}_4\text{PF}_6$  /  $\text{CH}_2\text{Cl}_2$  at 298 K. A 1.6 mm Pt disk electrode was used as the working electrode, a platinum wire was used as the auxiliary electrode, and a silver wire was used as a pseudo-reference electrode. Potentials were calibrated against the  $\text{Cp}^*\text{Fe}^{0/+}$  couple, which is known to occur at 0.548V vs the  $\text{Cp}_2\text{Fe}^{0/+}$  couple for this solvent medium.<sup>[44]</sup> The potentials in this paper can be changed to SCE reference values by addition of 0.56 V. Voltammograms were collected at 0.05 – 1.6 V/s with an EG&G PAR 263A potentiostat interfaced to a computer operated with EG&G PAR Model 270 software.

#### **X-ray Structure Determination for $[\text{RuCl}(\text{ind})(\text{PPh}_3)\{\text{P}(\text{pyr})_3\}]$ ,**

**$[\text{RuCl}(\text{ind})\{\text{P}(\text{pyr})_3\}_2]$  and **7b**:** Crystals of appropriate dimension of the metal complexes were obtained by slow diffusion of hexanes into a  $\text{CH}_2\text{Cl}_2$  solution of the compounds and for **7b** obtained by layering an ethyl acetate solution of the compound with hexanes. Crystals were mounted on MiTeGen cryoloops in random orientations. Preliminary examination and data collection were performed using a Bruker X8 Kappa Apex II Charge Coupled Device (CCD) Detector system single crystal X-Ray diffractometer equipped with an Oxford Cryostream LT device. All data were collected using graphite monochromated Mo  $\text{K}\alpha$  radiation ( $\lambda = 0.71073 \text{ \AA}$ ) from a fine focus sealed tube X-Ray source. Preliminary unit cell constants were determined with a set of 36 narrow frame scans. Typical data sets consist of combinations of  $\omega$  and  $\Phi$  scan frames with typical scan width of  $0.5^\circ$  and counting time of 15 seconds/frame at a crystal to detector distance of 4.0 cm. The collected frames were

integrated using an orientation matrix determined from the narrow frame scans. Apex II and SAINT software packages were used for data collection and data integration.<sup>[45]</sup> Analysis of the integrated data did not show any decay. Final cell constants were determined by global refinement of reflections harvested from the complete data set. Collected data were corrected for systematic errors using SADABS based on the Laue symmetry using equivalent reflections.<sup>[45]</sup>

Crystal data and intensity data collection parameters are listed in Table 1. Structure solution and refinement were carried out using the SHELXTL- PLUS software package.<sup>[46]</sup> The structures were solved by direct methods and refined successfully in the space groups,  $P_{bca}$ ,  $P2_1/c$  and  $P\bar{1}$ , respectively for compounds  $[\text{RuCl}(\text{ind})(\text{PPh}_3)\{\text{P}(\text{pyr})_3\}]$ ,  $[\text{RuCl}(\text{ind})\{\text{P}(\text{pyr})_3\}_2]$ , and **7b**. Full matrix least-squares refinements were carried out by minimizing  $\sum w(F_o^2 - F_c^2)^2$ . The non-hydrogen atoms were refined anisotropically to convergence. All hydrogen atoms were treated using appropriate riding model (AFIX m3). The final residual values and structure refinement parameters are listed in Table 1.

**Supporting information.** Crystallographic data for the structural analysis has been deposited with the Cambridge Crystallographic Data Centre, CCDC No. 1053440 for compound **7b**, CCDC No. 1053441 for complex  $[\text{RuCl}(\text{ind})\{\text{P}(\text{pyr})_3\}_2]$ , and CCDC No. 1053442 for complex  $[\text{RuCl}(\text{ind})(\text{PPh}_3)\{\text{P}(\text{pyr})_3\}]$ . Copies of this information may be obtained free of charge via <http://www.ccdc.cam.ac.uk>. Supporting information (experimental details for the known catalysis products in Table 3, NMR spectra ( $^1\text{H}$ ,  $^{13}\text{C}$ ) for

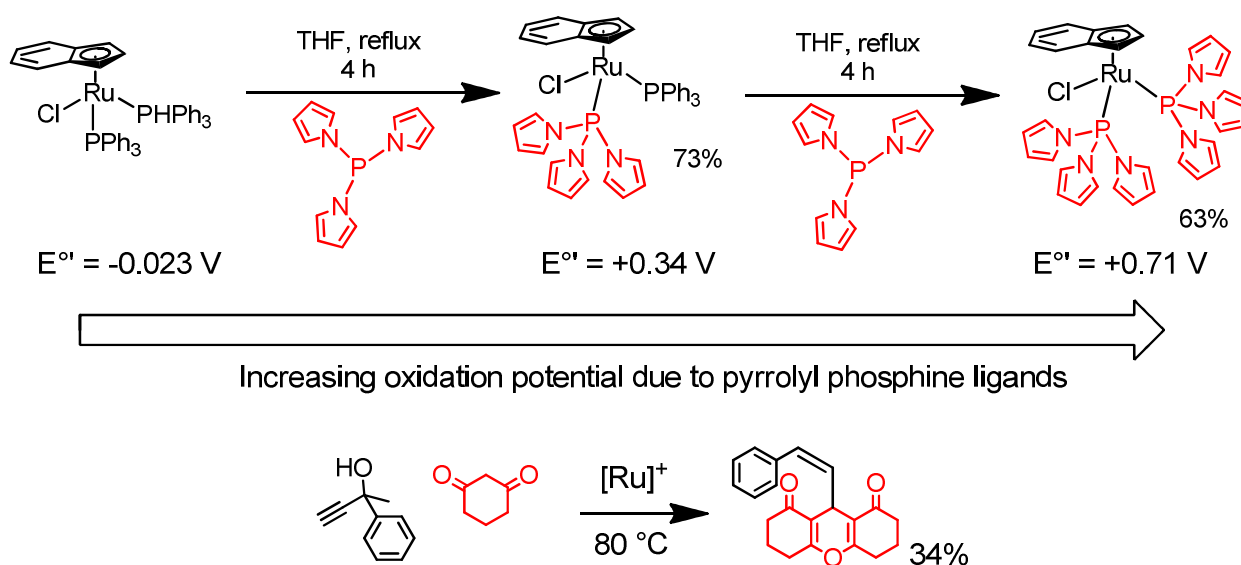
the metal complexes  $[\text{RuCl}(\text{ind})(\text{PPh}_3)\{\text{P}(\text{pyr})_3\}]$  and  $[\text{RuCl}(\text{ind})\{\text{P}(\text{pyr})_3\}_2]$  and all catalysis products) can be found as pdf-document in the online version of this article.

## Acknowledgment

We would like to thank the National Science Foundation for financial support: Eike B. Bauer, NSF CHE-1300818 and Michael J. Shaw, CHE-1213680. Further funding from the National Science Foundation for the purchase of the NMR spectrometer (CHE-9974801), the ApexII diffractometer (MRI, CHE-0420497), and the mass spectrometer (CHE-9708640) is acknowledged.

## Table of Contents text and Graphical Abstract

Key Topic: **Electronic Tuning**





The ruthenium pyrrolyl phosphine complexes  $[\text{RuCl}(\text{ind})(\text{PPh}_3)\{\text{P}(\text{pyr})_3\}]$  and  $[\text{RuCl}(\text{ind})\{\text{P}(\text{pyr})_3\}_2]$  were synthesized, and exhibited increased oxidation potentials due to the  $\pi$ -acidic pyrrolyl phosphine ligands. The complexes are catalytically active in the etherification of propargylic alcohols and in the formation of known and new xanthenones from propargylic alcohols and diketones.

## References

- [1] a) I. Dragutan, V. Dragutan, A. Demonceau, *Molecules* **2015**, *20*, 17244–17274; b) P. Kumar, R. Kumar Gupta, D. Shankar Pandey, *Chem. Soc. Rev.* **2014**, *43*, 707–733; c) C. Bonaccorsi, A. Mezzetti, *Curr. Org. Chem.* **2006**, *10*, 225–240; d) K. Grela, A. Michrowska, M. Bieniek, *The Chemical Record* **2006**, *6*, 144–156; e) H. Schaffrath, W. Keim, *J. Mol. Catal. A* **2001**, *168*, 9–14.
- [2] a) G. C. Vougioukalakisa, A. I. Philippopoulosb, T. Stergiopoulousa, P. Falarasa, *Coord. Chem. Rev.* **2011**, *255*, 2602–2621; b) S. Fantacci, F. De Angelis, *Coord. Chem. Rev.* **2011**, *255*, 2704–2726; c) K. Heinze, K. Hempel, A. Breivogel, *Z. Anorg. Allg. Chem.* **2009**, *635*, 2541–2549.
- [3] Representative examples: a) R. F. S. Lee, S. Escrig, M. Croisier, S. Clerc-Rosset, G. W. Knott, A. Meibom, C. A. Davey, K. Johnsson, P. J. Dyson, *Chem. Commun.* **2015**, *51*, 16486–16489; b) R. Trondl, P. Heffeter, C. R. Kowol, M. A. Jakupec, W. Berger, B. K. Keppler, *Chem. Sci.* **2014**, *5*, 2925–2932; c) N. A. Vyas, S. S. Bhat, A. S. Kumbhar, U.B. Sonawane, V. Jani, R. R. Joshi, S. N. Ramteke, P. P. Kulkarni, B. Joshi, *Eur. J. Med. Chem.*

**2014**, *75*, 375–381; d) A. Wragg, M. R. Gill, D. Turton, H. Adams, T. M. Roseveare, C. Smythe, X. Su, J. A. Thomas, *Chem. Eur. J.* **2014**, *20*, 14004–14011; e) Erwin Reisner, V. B. Arion, B. K. Keppler, A. J.L. Pombeiro, *Inorg. Chim. Act.* **2008**, *361*, 1569–1583.

[4] M. J. Clarke, *Coord. Chem. Rev.* **2003**, *236*, 209–233

[5] a) R. H. Morris, *Acc. Chem. Res.* **2015**, *48*, 1494–1502; b) L. Delaude, A. Demonceau, *Dalton Trans.* **2012**, *41*, 9257–9268; c) A. Mezzetti, *Dalton Trans.* **2010**, *39*, 7851–7869.

[6] Representative examples: a) B. Yu, Y. Xie, F. B. Hamad, K. Leus, A. A. Lyapkov, K. Van Hecke, F. Verpoort, *New J. Chem.* **2015**, *39*, 1858–1867; b) R. Staehle, L. Tong, L. Wang, L. Duan, A. Fischer, M. S. G. Ahlquist, L. Sun, S. Rau, *Inorg. Chem.* **2014**, *53*, 1307–1319; c) S. Enthaler, R. Jackstell, B. Hagemann, K. Junge, G. Erre, M. Beller, *J. Organomet. Chem.* **2006**, *691*, 4652–4659.

[7] Representative examples: a) T. Glöge, K. Jess, T. Bannenberg, P. G. Jones, N. Langenscheidt-Dabringhausen, A. Salzer, M. Tamm, *Dalton Trans.* **2015**, *44*, 11717–11724; b) B. Kali Dey, J. Dutta, M. G. B. Drew, S. Bhattacharya, *J. Organomet. Chem.* **2014**, *750*, 176–184.

[8] C. A. Fleckenstein, H. Plenio, *Chem. Soc. Rev.* **2010**, *39*, 694–711.

[9] K. G. Moloy, J. L. Petersen, *J. Am. Chem. Soc.* **1995**, *117*, 7696–7710.

[10] See for example: a) R. Menye-Biyogo, F. Delpech, A. Castel, V. Pimienta, H. Gornitzka, P. Rivière, *Organometallics* **2007**, *26*, 5091–5101; b) I. Angurell, I. Martínez-Ruiz, O. Rossell, M. Seco, P. Gómez-Sal, A. Martín, M. Font-Bardia, X. Solans, *J. Organomet. Chem.* **2007**, *692*, 3882–3891; c) I. Angurell, I. Martínez-Ruiz, O. Rossell, M.

Seco, P. Gómez-Salb, A. Martín, *Chem. Commun.* **2004**, 1712 – 1713; d) K. N. Gavrilov, V. N. Tsarev, S. I. Konkin, S. E. Lyubimov, A. A. Korlyukov, M. Yu. Antipin, V. A. Davankov, *Eur. J. Inorg. Chem.* **2005**, 3311–3319; e) A. D. Burrows, M. F. Mahon, M. T. Palmer, M. Varrone, *Inorg. Chem.* **2002**, *41*, 1695–1697; f) C. E.F. Rickard, W. R. Roper, S. D. Woodgate, L. J. Wright, *J. Organomet. Chem.* **2002**, *643–644*, 168–173; g) R. Jackstell, H. Klein, M. Beller, K.-D. Wiese, D. Röttger, *Eur. J. Org. Chem.* **2001**, 3871–3877.

[11] N. A. Foley, M. Lail, T. B. Gunnoe, T. R. Cundari, P. D. Boyle, J. L. Petersen, *Organometallics* **2007**, *26*, 5507–5516.

[12] a) A. D. Burrows, R. W. Harrington, M. F. Mahon, M. T. Palmer, F. Senia, M. Varrone, *Dalton Trans.* **2003**, 3717–3726; b) A. D. Burrows, M. F. Mahon, M. Varrone, *Inorg. Chim. Act.* **2003**, *350*, 152–162; c) A. Huang, J. E. Marcone, K. L. Mason, W. J. Marshall, K. G. Moloy, S. Serron, S. P. Nolan, *Organometallics* **1997**, *16*, 3377–3380.

[13] a) S. Costin, N. P. Rath, E. B. Bauer, *Inorg. Chem. Commun.* **2011**, 478–480; b) F. Delpéch, S. Sabo-Etienne, J.-C. Daran, B. Chaudret, K. Hussein, C. J. Marsden, J.-C. Barthelat, *J. Am. Chem. Soc.* **1999**, *121*, 6668–6682; c) V. Rodriguez, B. Donnadieu, S. Sabo-Etienne, B. Chaudret, *Organometallics* **1998**, *17*, 3809–3814; d) C. Li, S. Serron, S. P. Nolan, *Organometallics* **1996**, *15*, 4020–4029.

[14] E. B. Bauer, *Synthesis* **2012**, 1131–1151,

[15] a) M. J. Queensen, J. M. Rabus, E. B. Bauer, *J. Mol. Cat. A: Chem.* **2015**, *407*, 221–229; b) M. J. Queensen, N. P. Rath, E. B. Bauer, *Organometallics* **2014**, 5052–5065; c) D. F. Alkhaleeli, K. J. Baum, J. M. Rabus, E. B. Bauer, *Catal. Commun.* **2014**, *47*, 45–48; d) A. K. Widaman, N. P. Rath, E. B. Bauer, *New J. Chem.* **2011**, *35*, 2427–2434; e) S. Costin,

A. K. Widaman, N. P. Rath, E. B. Bauer, *Eur. J. Inorg. Chem.* **2011**, 1269–1282; f) S. Costin, N. P. Rath, E. B. Bauer, *Tetrahedron Lett.* **2009**, *50*, 5485–5488; g) S. Costin, S. L. Sedinkin, E. B. Bauer, *Tetrahedron Lett.* **2009**, *50*, 922–925; h) S. Costin, N. P. Rath, E. B. Bauer, *Adv. Synth. Catal.* **2008**, *350*, 2414–2424.

[16] Representative examples of ruthenium-catalyzed transformations of propargylic alcohols: a) J. Jeschke, C. Gäbler, M. Korb, T. Ruffer, H. Lang, *Eur. J. Inorg. Chem.* **2015**, 2939–2947; b) Y. Senda, K. Nakajima, Y. Nishibayashi, *Angew. Chem. Int. Ed.* **2015**, *54*, 4060–4064; c) C. Schreiner, J. Jeschke, B. Milde, D. Schaarschmidt, H. Lang, *J. Organomet. Chem.* **2015**, *785*, 32–43; d) N. Thies, E. Haak, *Angew. Chem. Int. Ed.* **2015**, *54*, 4097–4101; e) G. C. Tsui, K. Villeneuve, E. Carlson, W. Tam, *Organometallics* **2014**, *33*, 3847–3856; f) N. Thies, M. Gerlach, E. Haak, *Eur. J. Org. Chem.* **2013**, 7354–7365; g) N. P. Hiatt, J. M. Lynam, C. E. Welby, A. C. Whitwood, *J. Organomet. Chem.* **2011**, *696*, 378–387; h) V. Cadierno, J. Francos, J. Gimeno, *Organometallics* **2011**, *30*, 852–862; i) V. Cadierno, J. Francos, J. Gimeno, *Green Chem.* **2010**, *12*, 135–143; j) V. Cadierno, J. Gimeno, N. Nebra, *Adv. Synth. Catal.* **2007**, *349*, 382–394; k) V. Cadierno, S. E. García-Garrido, J. Gimeno, *Adv. Synth. Catal.* **2006**, *348*, 101–110.

[17] Reviews: a) V. Cadierno, J. Gimeno, *Chem. Rev.* **2009**, *109*, 3512–3560; b) C.-M. Che, C.-M. Ho, J. S. Huang, *Coord. Chem. Rev.* **2007**, *251*, 2145–2166; c) R. F. Winter, S. Zális, *Coord. Chem. Rev.* **2004**, *248*, 1565–1583; d) S. Rigaut, D. Touchard, P. H. Dixneuf, *Coord. Chem. Rev.* **2004**, *248*, 1585–1601; e) V. Cadierno, M. P. Gamasa, J. Gimeno, *Eur. J. Inorg. Chem.* **2001**, 571–591; f) M. I. Bruce, *Chem. Rev.* **1998**, *98*, 2797–2858; g) H. Werner, *Chem. Commun.* **1997**, 903–310.

- [18] L. A. Oro, M. A. Ciriano, M. Campo, C. Foces-Foces, F. H. J. Cano, *J. Organomet. Chem.* **1985**, 289, 117–131.
- [19] a) M. Pilar Gamasa, J. Gimeno, C. Gonzalez-Bernardo, B. M. Martín-Vaca, D. Monti, M. Bassetti, *Organometallics* **1996**, 15, 302–308; b) V. Cadierno, J. Díez, M. Pilar Gamasa, J. Gimeno, E. Lastra, *Coord. Chem. Rev.* **1999**, 193–195, 147–205.
- [20] a) S. Nolan, *Acc. Chem. Res.* **2014**, 47, 3089–3101; b) Charles A. Mebi, Radhika P. Nair, and Brian J. Frost, *Organometallics* **2007**, 26, 429–438; c) K. Bieger, J. Díez, M. Pilar Gamasa, J. Gimeno, M. Pavlišta, Y. Rodríguez-Álvarez, S. García-Granda, R. Santiago-García, *Eur. J. Inorg. Chem.* **2002**, 1647–1656; d) P. Alvarez, J. Gimeno, E. Lastra, S. García-Granda, J. F. Van der Maelen, M. Bassetti, *Organometallics* **2001**, 20, 3762–3771; e) E. P. Kündig, C. M. Saudan, V. Alezra, F. Viton, G. Bernardinelli, *Angew. Chem. Int. Ed.* **2001**, 40, 4481–4485; f) M. Bassetti, S. Marini, F. Tortorella, V. Cadierno, J. Díez, M. Pilar Gamasa, J. Gimeno *J. Organomet. Chem.* **2000**, 593–594, 292–298; g) Y. Yamamoto, H. Kitahara, R. Hattori, K. Itoh *Organometallics* **1998**, 17, 1910–1912.
- [21] a) M. José Calhorda, L. F. Veiros, *Dalton Trans.* **2011**, 40, 11138–11146; b) M. José Calhorda, C. C. Romão, L. F. Veiros, *Chem. Eur. J.* **2002**, 8, 868–875; c) L. F. Veiros *Organometallics* **2000**, 19, 3127–3136; d) J. M. O'Connor, C. P. Casey, *Chem. Rev.* **1987**, 87, 307–318; e) J. W. Faller, R. H. Crabtree, A. Habib, *Organometallics* **1985**, 4, 929–935.
- [22] G. L. Gibson, K. M. E. Morrow, R. McDonald, L. Rosenberg, *Inorg. Chim. Act.* **2011**, 369, 133–139.
- [23] E. J. Derrah, J. C. Marlinga, D. Mitra, D. M. Friesen, S. A. Hall, R. McDonald, L. Rosenberg, *Organometallics* **2005**, 24, 5817–5827.

- [24] M. Kamigaito, Y. Watanabe, T. Ando, M. Sawamoto, *J. Am. Chem. Soc.* **2002**, *124*, 9994–9995.
- [25] a) J. Lodinský, J. Vinklárek, L. Dostál, Z. Růžičková, J. Honzíček, *RSC Adv.* **2015**, *5*, 27140–27153; b) J. Honzíček, J. Vinklárek, M. Erben, J. Lodinský, L. Dostál, Z. Padělkova, *Organometallics* **2013**, *32*, 3502–3511.
- [26] a) R. P. Pinnell, C. A. Megerle, S. L. Manatt, P. A. Kroon, *J. Am. Chem. Soc.* **1973**, *95*, 977–978; b) R. D. Kroshefsky, R. Weiss, J. G. Verkade, *Inorg. Chem.* **1979**, *18*, 469–472; c) A. Suárez, M. A. Méndez-Rojas, A. Pizzano, *Organometallics* **2002**, *21*, 4611–4621; d) S. Jeulin, S. Duprat de Paule, V. Ratovelomanana-Vidal, J.-P. Genêt, N. Champion, P. Dellis, *Angew. Chem. Int. Ed.* **2004**, *43*, 320 320–325; e) V. Bilenko, A. Spannenberg, W. Baumann, I. Komarov, A. Börner, *Tetrahedron: Asymmetry* **2006**, *17*, 2082-2087; f) D. J. Adams, J.A. Bennett, D. Duncan, E. G. Hope, J. Hopewell, A. M. Stuart, A. J. West, *Polyhedron* **2007**, *26*, 1505–1513; g) S. Enthaler, G. Erre, K. Junge, K. Schröder, D. Addis, D. Michalik, M. Hapke, D. Redkin, M. Beller, *Eur. J. Org. Chem.* **2008**, 3352–3362; h) G. Erre, K. Junge, S. Enthaler, D. Addis, D. Michalik, A. Spannenberg, M. Beller, *Chem. Asian J.* **2008**, *3*, 887–894; i) P/ Shejwalkar, Sergey L. Sedinkin, E. B. Bauer *Inorg. Chim. Act.*, **2011**, *366*, 209–218.
- [27] T. S. Barnard, M. R. Mason, *Organometallics* **2001**, *20*, 206–214 .
- [28] a) B. Suthar, A. Aldongarov, I. S. Irgibaeva, M. Moazzen, B. T. Donovan-Merkert, J. W. Merkert, T. A. Schmedake, *Polyhedron* **2012**, *31*, 754–758; b) A. P. Shaw, J. R. Norton, D. Buccella, L. A. Sites, S. S. Kleinbach, D. A. Jarem, K. M. Bocage, C. Nataro,

*Organometallics* **2009**, *28*, 3804–3814; c) A. R. O'Connor, C. Nataro, A. L. Rheingold, *J. Organomet. Chem.* **2003**, *679*, 72–78.

[29] General examples and reviews regarding the nucleophilic substitution of propargylic alcohols: a) K. Nakajima, M. Shibata, Y. Nishibayashi *J. Am. Chem. Soc.* **2015**, *137*, 2472–2475; b) D.-Y. Zhang, X.-P. Hu, *Tetrahedron Lett.* **2015**, *56*, 283–295; c) B. Wang, C. Liu, H. Guo, *RSC Adv.* **2014**, *4*, 2014, 53216–53219; d) F.-Z. Han, F.-L. Zhu, Y.-H. Wang, Y. Zou, X.-H. Hu, S. Chen, X.-P. Hu, *Org. Lett.* **2014**, *16*, 588–591; e) Y. Nishibayashi, *Synthesis* **2012**, *44*, 489–503; f) R. J. Detz, H. Hiemstra, J. H. van Maarseveen, *Eur. J. Org. Chem.* **2009**, 6263–6276; g) N. Ljungdahl, N. Kann, *Angew. Chem. Int. Ed.* **2009**, *48*, 642–644.

[30] M. Picquet, C. Bruneau, P. H. Dixneuf, *Chem. Commun.* 1997, 1201–1202.

[31] A. L. Krasovskiy, S. Haley, K. Voigtritter, B. H. Lipshutz, *Org. Lett.* **2014**, *16*, 4066–4069.

[32] V. R. Narayana, Z. Pudukulathan, R. Varala, *Org. Commun.* **2013**, *6*, 110–119.

[33] G. M. Nazeruddin, A. A. Shaikh, Y. I. Shaikh, *Pharm. Lett.* **2011**, *3*, 193–197.

[34] R. Sanz, D. Miguel, A. Martínez, J. M. Álvarez-Gutiérrez, F. Rodríguez, *Org. Lett.* **2007**, *9*, 727–730.

[35] A. Ilangovan, S. Malayappasamy, S. Muralidharan, S. Maruthamuthu, *Chem. Cent. J.* **2011**, *5*, 81–87.

[36] K. Rohr, R. Mahrwald, *Bioorg. Med. Chem. Lett.* **2009**, *19*, 3949–3951.

[37] V. Cadierno, P. Crochet, S. E. García-Garrido, J. Gimeno, *Dalton Trans.* **2010**, 39, 4015–4031.

- [38] a) A. Pramanik, S. Bhar, *Catal. Commun.* **2012**, *20*, 17–24; b) J. Ma, X. Zhou, X. Zang, C. Wang, Z. Wang, J. Li, Q. Li, *Aust. J. Chem.* **2007**, *60*, 146–1481.
- [39] X. Fan, X. Hu, X. Zhang, J. Wang, *Can. J. Chem.* **2005**, *83*, 16–20.
- [40] N. Mulakayala, P.V.N.S. Murthy, D. Rambabu, M. Aeluri, R. Adepur, G. R. Krishna, C. Malla Reddy, K.R.S. Prasad, M. Chaitanya, C. S. Kumar, M.V. Basaveswara Rao, M. Pal, *Bioorg. Med. Chem. Lett.* **2012**, *22*, 2186–2191.
- [41] A. Arcadi, M. Alfonsi, M. Chiarini, F. Marinelli, *J. Organomet. Chem.* **2009**, *694*, 576–582.
- [42] a) F. Pünner, G. Hilt, *Chem. Commun.* **2012**, *48*, 3617–3619; b) B. Sathyamoorthy, A. Axelrod, V. Farwell, *Organometallics* **2010**, 3431–3441.
- [43] R. Riveiros, D. Rodríguez, J. Pérez Sestelo, L. A. Sarandeses, *Org. Lett.* **2006**, *8*, 1403–1406.
- [44] F. Barrière, W. E. Geiger, *J. Am. Chem. Soc.* **2006**, *128*, 3980–3989.
- [45] Bruker Analytical X-ray, Madison, WI, **2012**.
- [46] G. M. Sheldrick, *Acta Crystallogr., Sect. A* **2008**, *64*, 112–122.